Role of plasma edge region in global stability on NSTX*

J. Menard (PPPL), Y.Q. Liu (CCFE)
R. Bell, S. Gerhardt (PPPL)
S. Sabbagh (Columbia University)
and the NSTX Research Team

52nd Annual Meeting of the APS DPP
November 8-12
Chicago, IL

*This work supported by US DoE contract DE-AC02-09CH11466

College W&M
Colorado Sch Mines
Columbia U
CompX
General Atomics
INL
Johns Hopkins U
LANL
LLNL
Lodestar
MIT
Nova Photonics
New York U
Old Dominion U
ORNL
PPPL
PSI
Princeton U
Purdue U
SNL
Think Tank, Inc.
UC Davis
UC Irvine
UCLA
UCSD
U Colorado
U Illinois
U Maryland
U Rochester
U Washington
U Wisconsin

Culham Sci Ctr
U St. Andrews
York U
Chubu U
Fukui U
Hiroshima U
Hyogo U
Kyoto U
Kyushu U
Kyushu Tokai U
NIFS
Niigata U
U Tokyo
JAEA
Hebrew U
Ioffe Inst
RRC Kurchatov Inst
TRINITI
KBSI
KAIST
POSTECH
ASIPP
ENEA, Frascati
CEA, Cadarache
IPP, Jülich
IPP, Garching
ASCR, Czech Rep
U Quebec

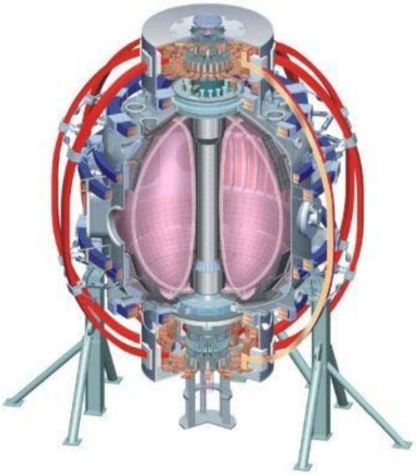

Outline

1. Experimental motivation

2. Role of E×B drift frequency profile

3. Kinetic stability analysis using MARS code
    - Comparisons with experiment
    - Self-consistent vs. perturbative approach

Error field correction (EFC) often necessary to maintain rotation, stabilize n=1 resistive wall mode (RWM) at high β_N

- No EFC → n=1 RWM unstable
- With EFC → n=1 RWM stable

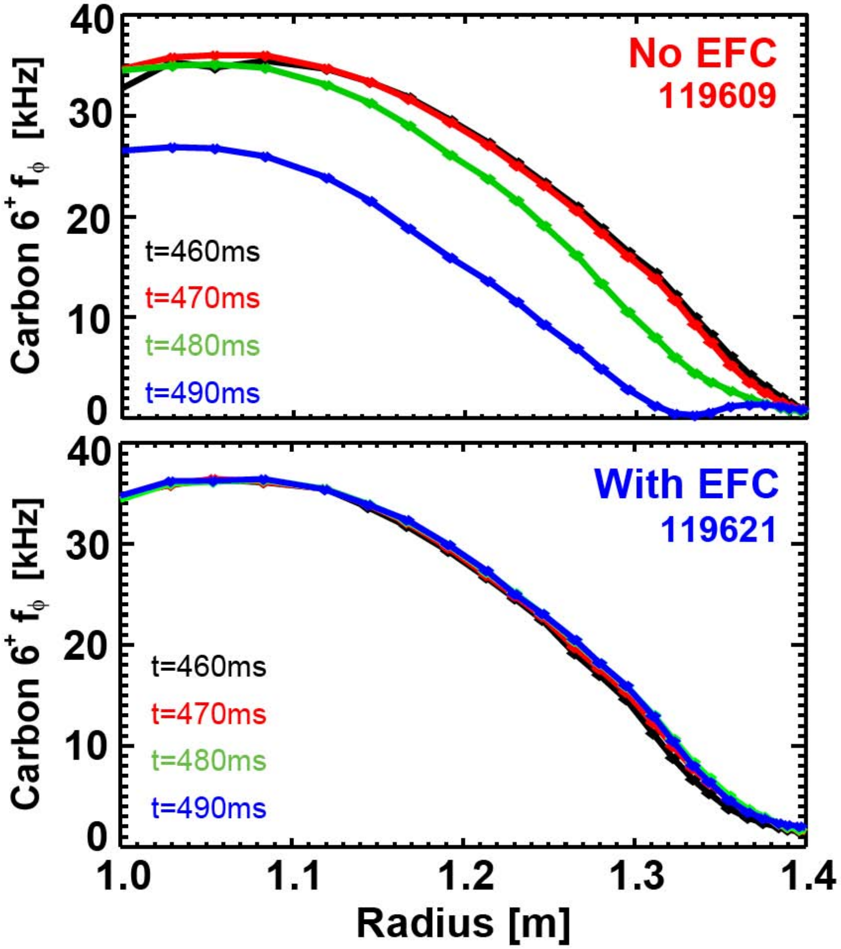

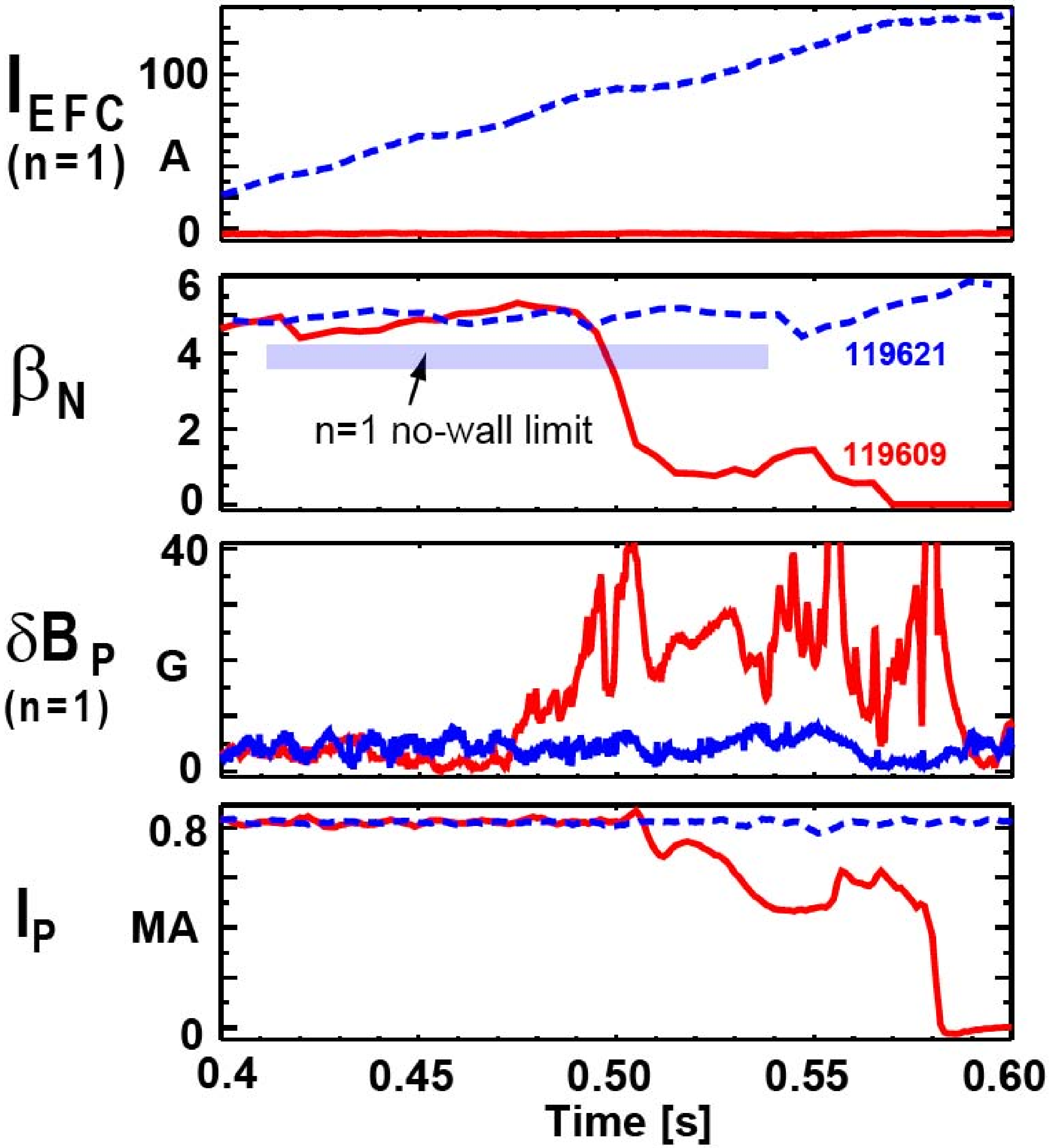

J.E. Menard et al, Nucl. Fusion 50 (2010) 045008

EFC experiments show edge region with q ≥ 4 and r/a ≥ 0.8 apparently determine stability

- **n=3 EFC → stable**
- **No EFC → n=1 RWM unstable**

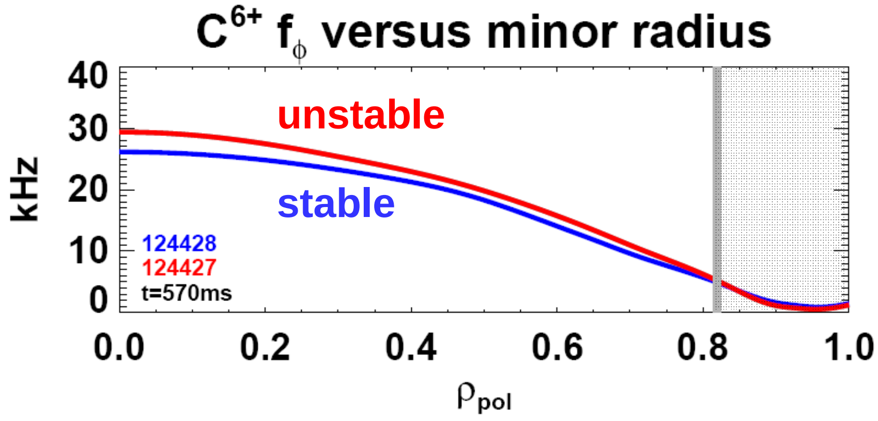

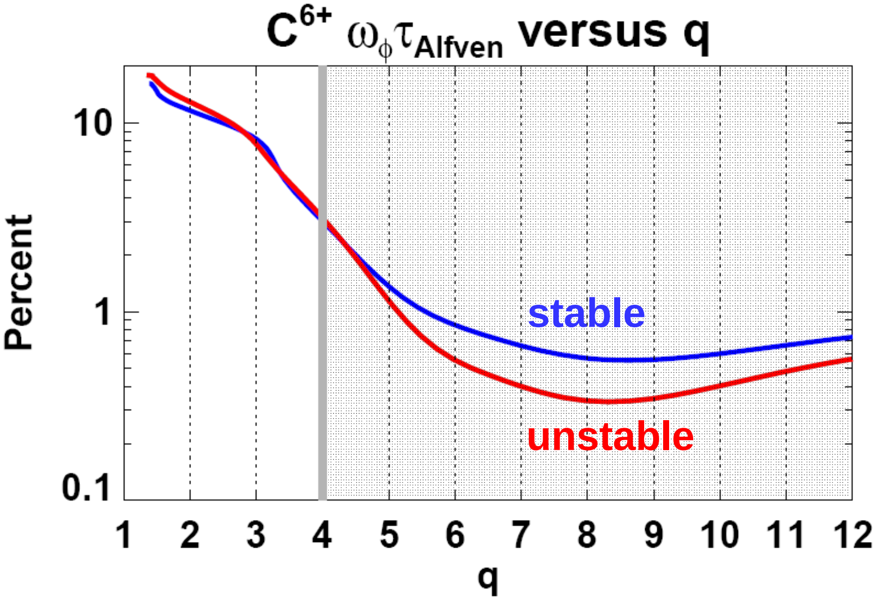

- **n=1 EFC →stable**
- **No EFC → n=1 RWM unstable**

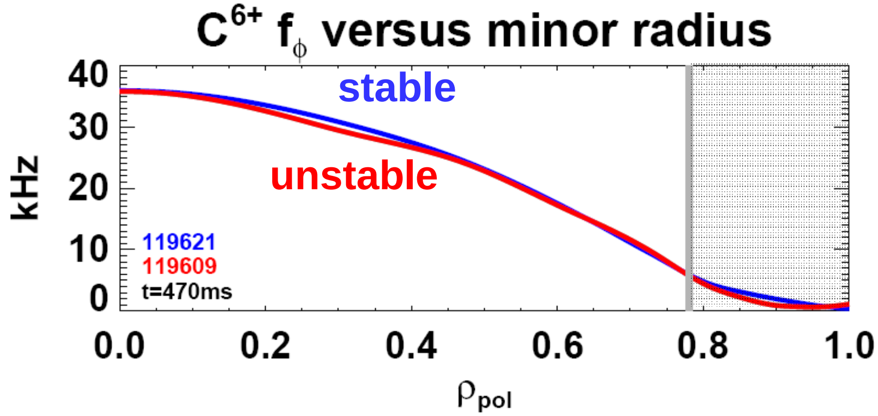

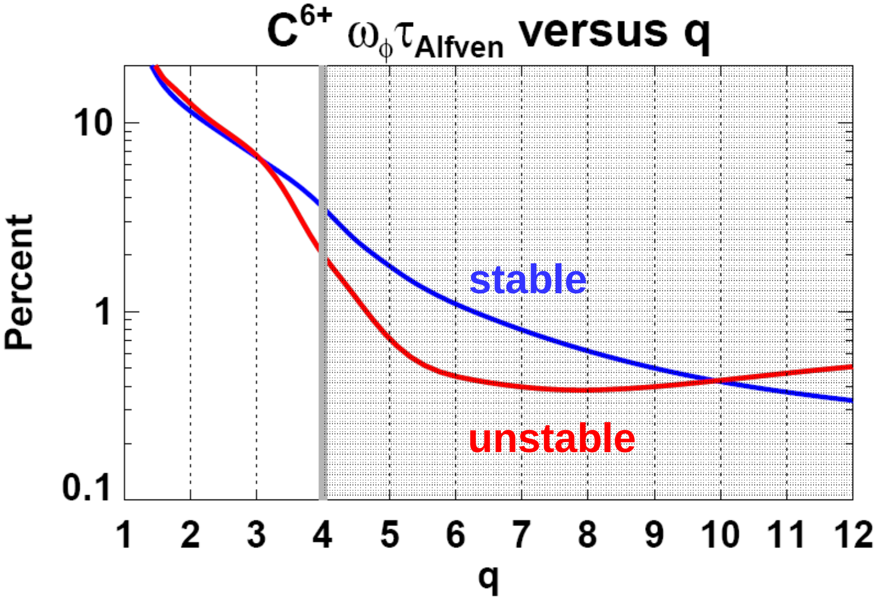

MARS is linear MHD stability code that includes toroidal rotation and drift-kinetic effects

- **Single-fluid linear MHD**

$$(\gamma + in\Omega)\boldsymbol{\xi} = \mathbf{v} + (\boldsymbol{\xi}\cdot\nabla\Omega)R^2\nabla\phi$$

$$\rho(\gamma + in\Omega)\mathbf{v} = -\nabla\cdot\mathbf{p} + \mathbf{j}\times\mathbf{B} + \mathbf{J}\times\mathbf{Q} - \rho[2\Omega\hat{\mathbf{Z}}\times\mathbf{v} + (\mathbf{v}\cdot\nabla\Omega)R^2\nabla\phi]$$

$$(\gamma + in\Omega)\mathbf{Q} = \nabla\times(\mathbf{v}\times\mathbf{B}) + (\mathbf{Q}\cdot\nabla\Omega)R^2\nabla\phi$$

$$(\gamma + in\Omega)p = -\mathbf{v}\cdot\nabla P, \qquad \mathbf{j} = \nabla\times\mathbf{Q}$$

Y.Q. Liu, et al., Phys. Plasmas 15, 112503 2008

- **Kinetic effects in perturbed *p*:**

$$\mathbf{p} = p\mathbf{I} + p_{\|}\hat{\mathbf{b}}\hat{\mathbf{b}} + p_{\perp}(\mathbf{I} - \hat{\mathbf{b}}\hat{\mathbf{b}})$$

$$p_{\|}e^{-i\omega t + in\phi} = \sum_{e,i}\int d\Gamma M v_{\|}^2 f_L^1$$

$$p_{\perp}e^{-i\omega t + in\phi} = \sum_{e,i}\int d\Gamma \frac{1}{2} M v_{\perp}^2 f_L^1$$

$$f_L^1 = -f_{\epsilon}^0 \epsilon_k e^{-i\omega t + in\phi}\sum X_m^u H_{ml}^u \lambda_{ml} e^{-in\tilde{\phi}(t) + im\langle\dot{\chi}\rangle t + il\omega_b t}$$

$$H_L = \frac{1}{\epsilon_k}[M v_{\|}^2 \vec{\kappa}\cdot\boldsymbol{\xi}_{\perp} + \mu(Q_{L\|} + \nabla B\cdot\boldsymbol{\xi}_{\perp})]$$

- **Mode-particle resonance operator:**

MARS-K:

$$\lambda_{ml} = \frac{n[\omega_{*N} + (\hat{\epsilon}_k - 3/2)\omega_{*T} + \omega_E] - \omega}{n(\langle\omega_d\rangle + \omega_E) + [\alpha(m + nq) + l]\omega_b - i\nu_{\text{eff}} - \omega}$$

MARS-F:

$$\lambda_{ml} = \frac{n[\cancel{\omega_{*N}} + (\hat{\epsilon}_k - 3/2)\cancel{\omega_{*T}} + \boxed{\omega_E] - \omega}}{n(\cancel{\langle\omega_d\rangle +} \boxed{\omega_E}) + [\alpha(m + nq) + l]\boxed{\omega_b} \cancel{- i\nu_{\text{eff}}} - \boxed{\omega}}$$

+ additional approximations/simplifications in f_L^1

- **Fast ions: MARS-K: slowing-down f(v), MARS-F: lumped with thermal**

Sensitivity of stability to rotation motivates study of all components of E×B drift frequency $\omega_E(\psi)$

- Decompose flow of species *j* into poloidal + toroidal components:

$$\vec{u}_j = u_{\theta j}(\psi)\vec{B}_P + \Omega_{\phi j}(\psi,\theta)R^2\nabla\phi \qquad \text{satisfying} \quad \nabla\cdot\vec{u}_j = 0$$

- Orbit-average E×B drift frequency: $\omega_E \equiv \langle\langle \vec{v}_E \cdot \nabla(\phi - q\theta)\rangle\rangle$

Bounce average: $\langle\langle X \rangle\rangle \equiv \frac{1}{\tau_b}\oint X d\tau$

$\vec{v}_E$ = E×B drift velocity

F. Porcelli, et al., Phys. Plasmas 1 (1994) 470

- Ignoring centrifugal effects (ok in plasma edge), ω_E reduces to:

1. parallel/toroidal **2. diamagnetic** **3. poloidal**

$$\boxed{\omega_E(\psi) = \frac{\langle\vec{u}_j\cdot\vec{B}\rangle}{F} - \omega_{*j} - u_{\theta j}(\psi)\frac{\langle B^2\rangle}{F}}$$

measured measured or neoclassical theory

$$\frac{\langle\vec{u}_j\cdot\vec{B}\rangle}{F} = \Omega_{\phi j}(\psi,\theta) + \frac{u_{\theta j}(\psi)}{F}\underbrace{\left[\langle B^2\rangle - \frac{F^2}{R^2}\right]}_{\text{reconstructions}}$$

flux function measured

Y.B. Kim, et al., Phys. Fluids B 3 (1991) 2050

Flux-surface average:

$\langle X \rangle \equiv \oint JXd\theta / \oint Jd\theta$

$F(\psi) \equiv RB_\phi$

NSTX edge v_{pol} ≈ neoclassical (within factor of ~2)

$B_T = 0.34T$

$V_{pol} \propto 1/B$ – trend
consistent with neoclassical

$B_T = 0.54T$

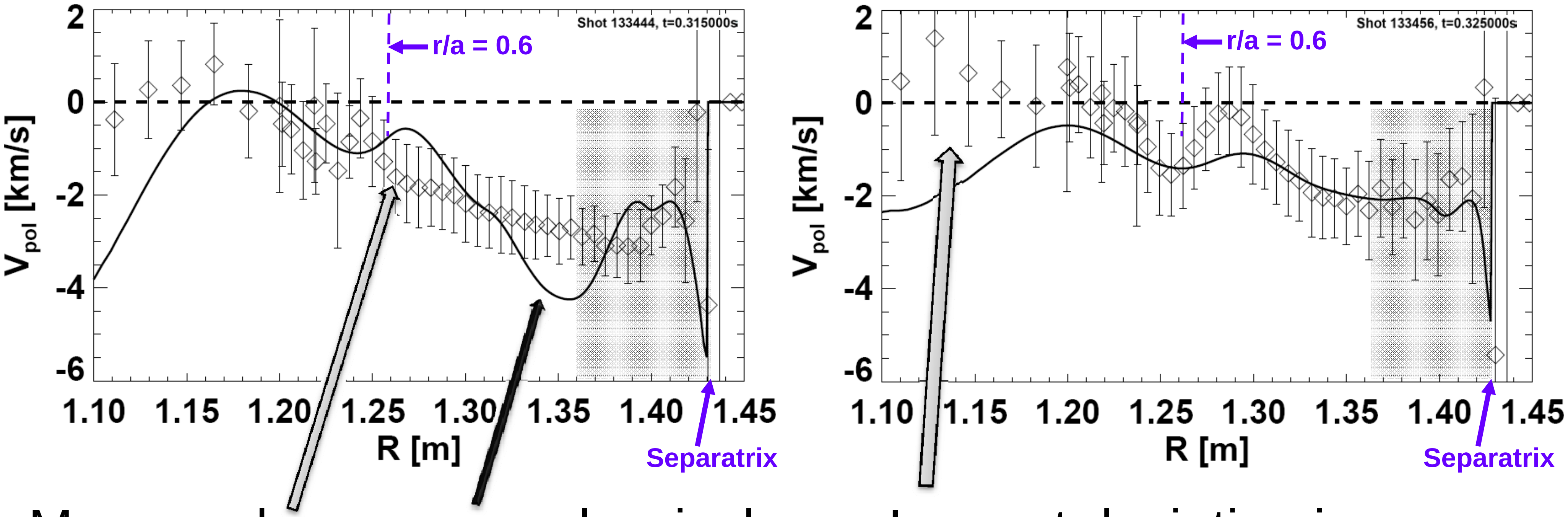

Measured v_{pol} neoclassical Largest deviation in core

Subsequent MARS calculations use neoclassical v_{pol}, but $v_{pol} = 0$ for r/a < 0.6

NSTX results: *R. E. Bell, et al., Phys. Plasmas **17**, 082507 (2010)*
Neoclassical: *W. Houlberg, et al., Phys. Plasmas **4**, 3230 (1997)*

n=1 EFC profiles show impurity C diamagnetic and poloidal rotation modify $|\omega_E \tau_A|$ ~ 1% in edge → potentially important

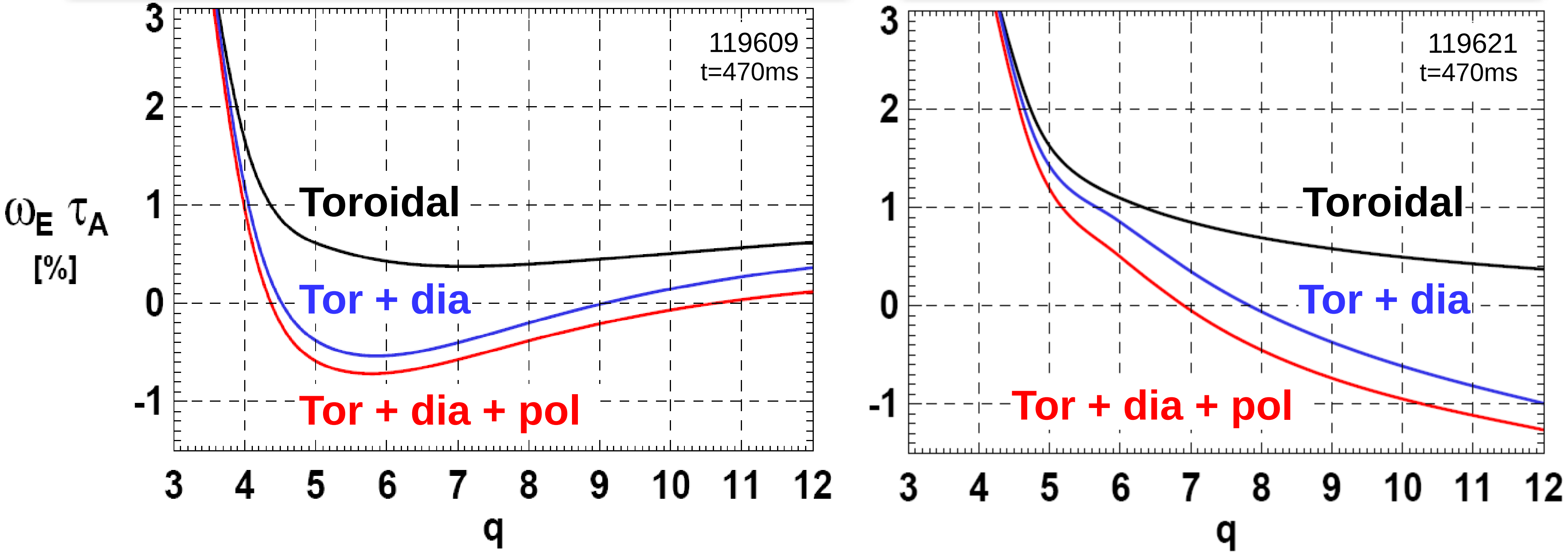

n=1 RWM unstable (no n=1 EFC)

n=1 RWM stable (n=1 EFC)

C^{6+} Toroidal rotation only: $\omega_E = \Omega_{\phi\text{-}C}(\psi)$

Toroidal + diamagnetic: $\omega_E = \Omega_{\phi\text{-}C}(\psi) - \omega_{*C}$

Toroidal + diamagnetic + poloidal: $\omega_E = \langle u_C \cdot B \rangle / F - \omega_{*C} - u_{\theta\text{-}C} \langle B^2 \rangle / F$

- Diamagnetic contribution to $\omega_E \tau_A$ ≈ -0.5 to -1.0%
- Neoclassical v_{pol} contribution to $\omega_E \tau_A$ ≈ -0.2 to -0.4%

A range of edge ω_E profile shapes can be stable, but unstable profiles can often be nearby

Toroidal + diamagnetic + poloidal

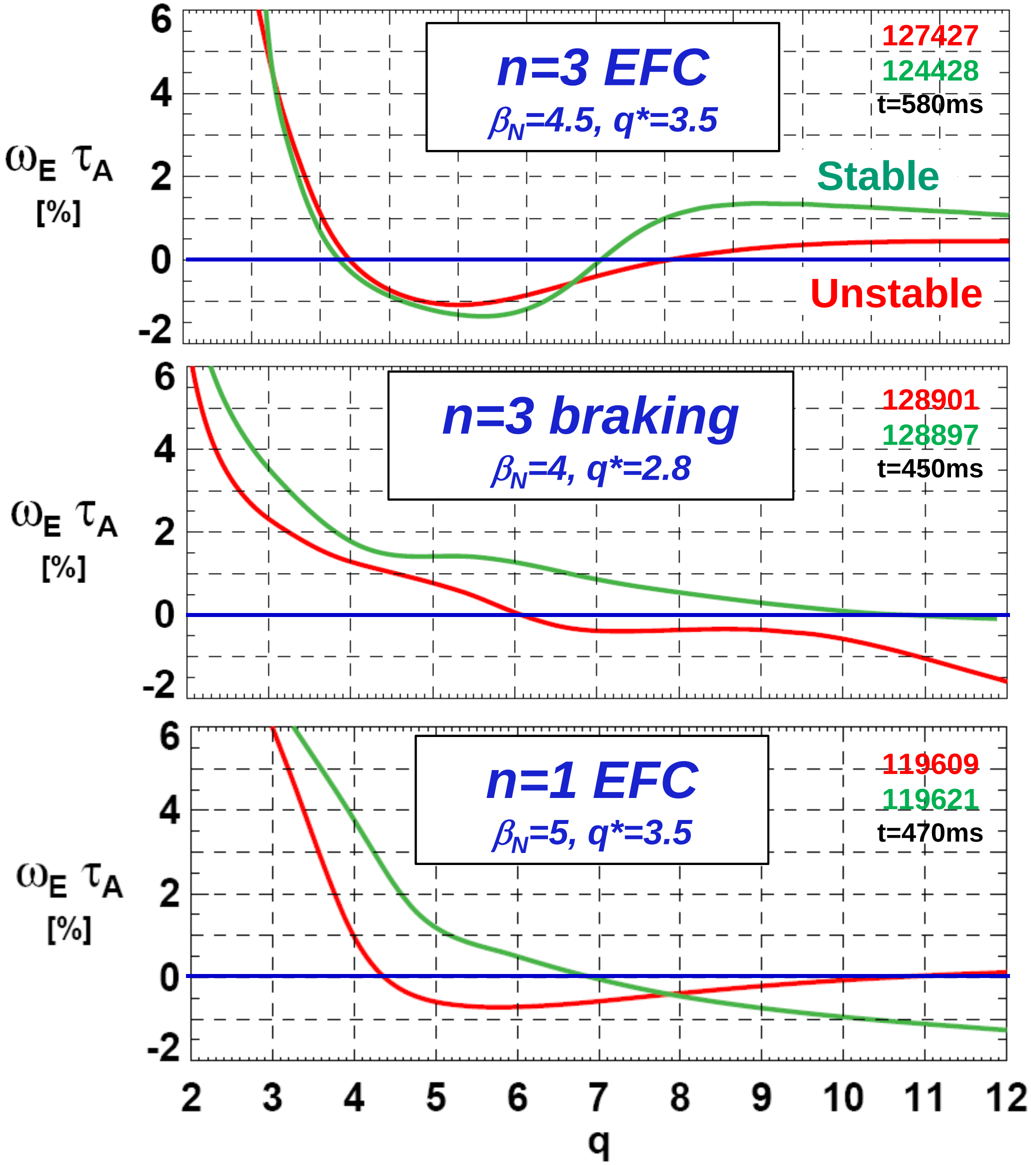

- Separation between **stable** and **unstable** profiles typically small: $\Delta(\omega_E\tau_A) \leq$ **1%**
- $\omega_E \approx 0$ over most of edge may correlate with instability
- Edge ω_E (r) control could potentially provide RWM stabilization technique
- Motivation for RWM active feedback control remains

Kinetic stability analysis using MARS-F

➡ ▪ Experimentally unstable case

- Experimentally stable case

- Comparison of unstable and stable cases

MARS-F using marginally unstable $\omega_E = \Omega_{\phi\text{-}C}$ predicts n=1 RWM to be robustly unstable → inconsistent with experiment

$$C_\beta \equiv \frac{\beta_N - \beta_N\,(\text{no-wall})}{\beta_N\,(\text{wall}) - \beta_N\,(\text{no-wall})}$$

Calculated n=1 $\gamma\tau_{wall}$

Using experimentally marginally unstable profiles

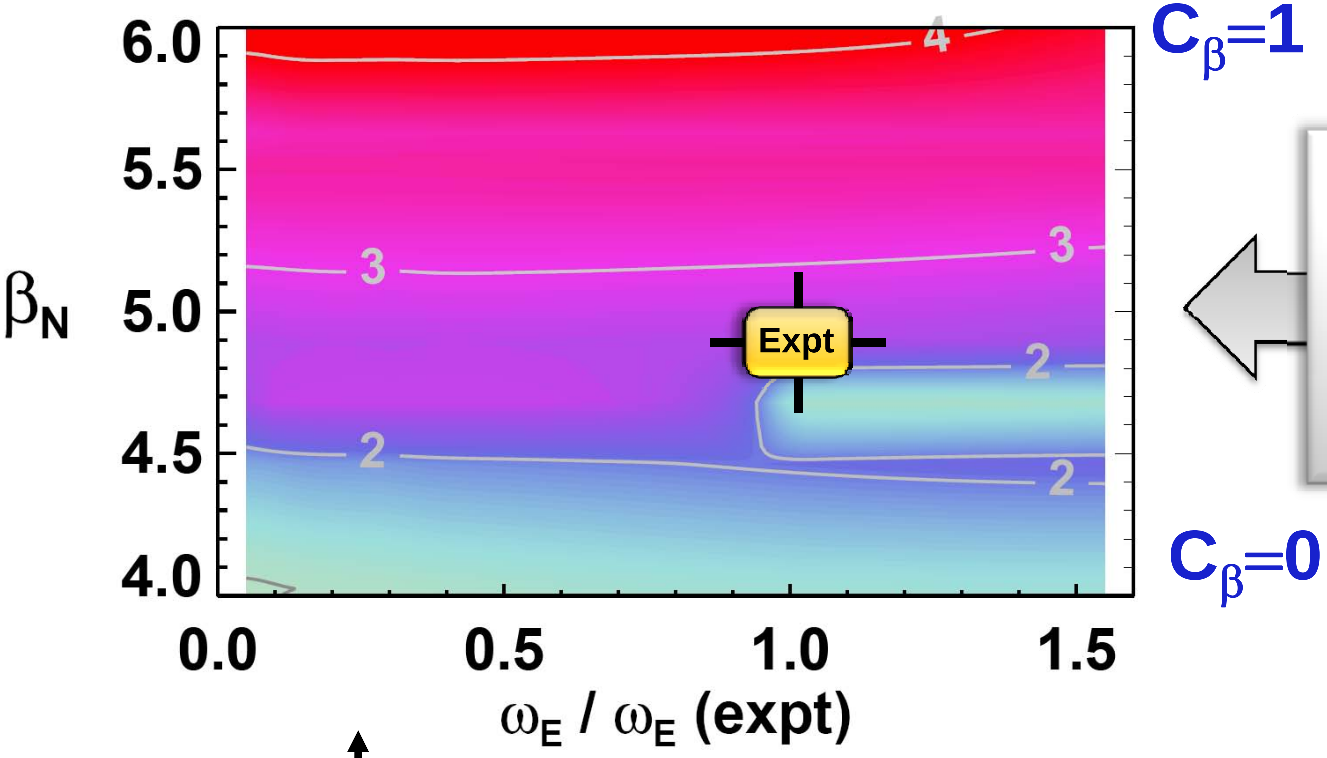

- γ depends only weakly on rotation
- γ increases with β_N

ω_{*C} / ω_{*C} (expt) = 0, u_θ = 0

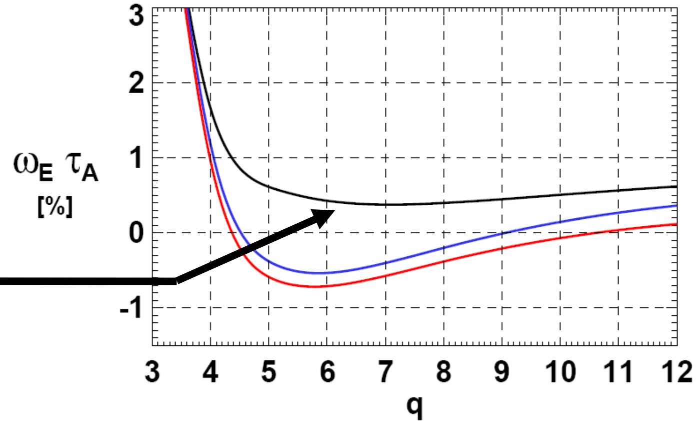

MARS-F using marginally unstable full ω_E predicts n=1 RWM to be marginally unstable → more consistent with experiment

Calculated n=1 $\gamma\tau_{wall}$

using experimentally marginally unstable profiles

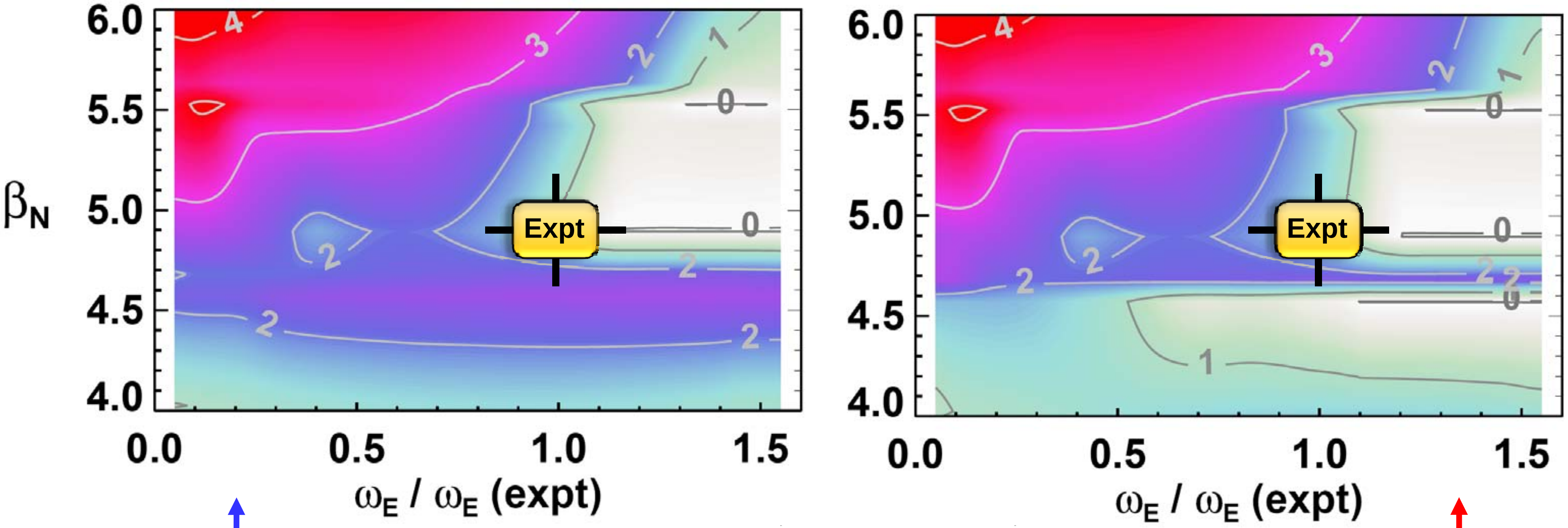

ω_{*C} / ω_{*C} (expt) = 1
u_θ = 0

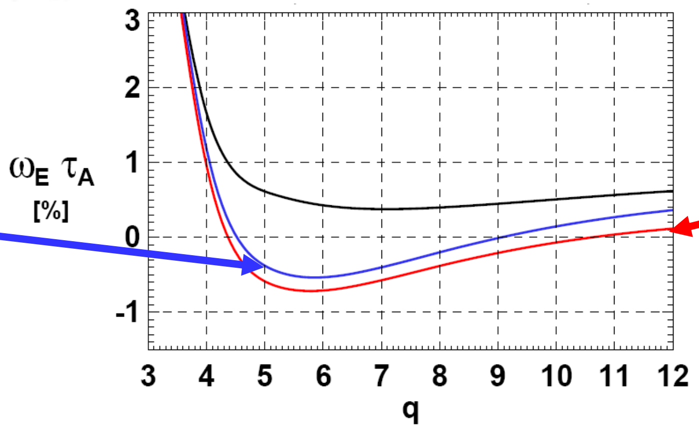

ω_{*C} / ω_{*C} (expt) = 1
u_θ = neoclassical

Kinetic stability analysis using MARS-F

- Experimentally unstable case
- ➡ Experimentally stable case
- Comparison of unstable and stable cases

MARS-F using stable $\omega_E = \Omega_{\phi\text{-}C}$ profile predicts n=1 RWM to be unstable → inconsistent with experiment

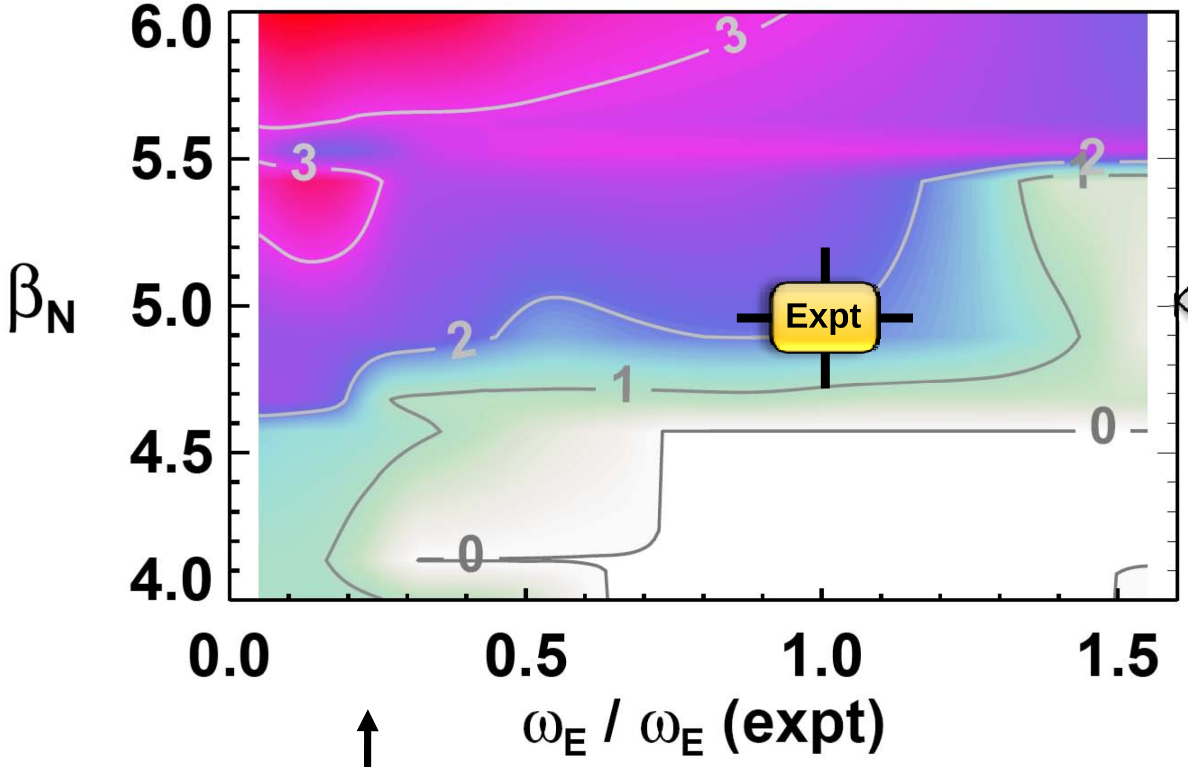

Calculated n=1 $\gamma\tau_{wall}$

using experimentally stable profiles

- **n=1 RWM predicted to be unstable for β_N > 4.6, but actual plasma operates stably at $\beta_N \geq 5$**

ω_{*C} / ω_{*C} (expt) = 0, u_θ = 0

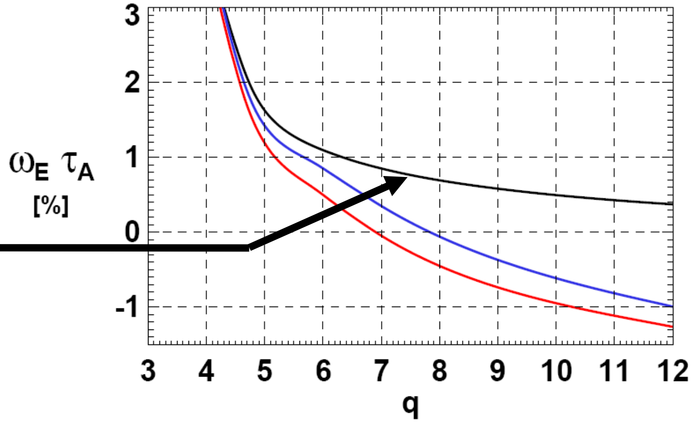

MARS-F using stable full ω_E profile predicts wide region of marginal stability → more consistent with experiment

Calculated n=1 $\gamma\tau_{wall}$

using experimentally stable profiles

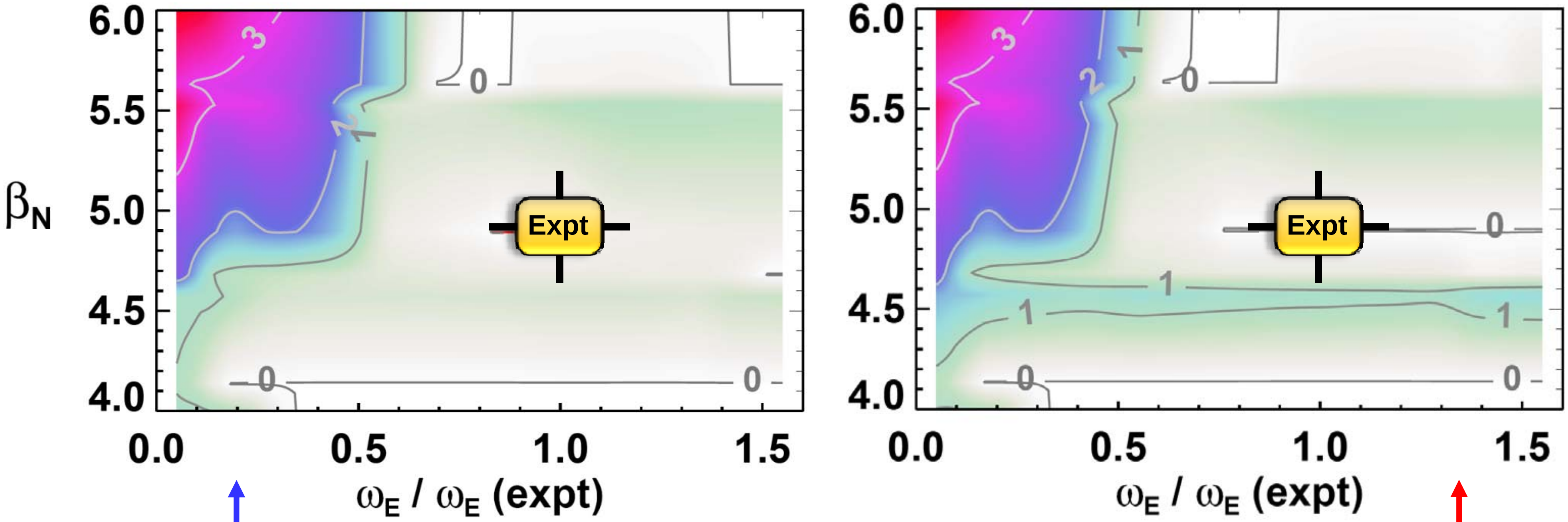

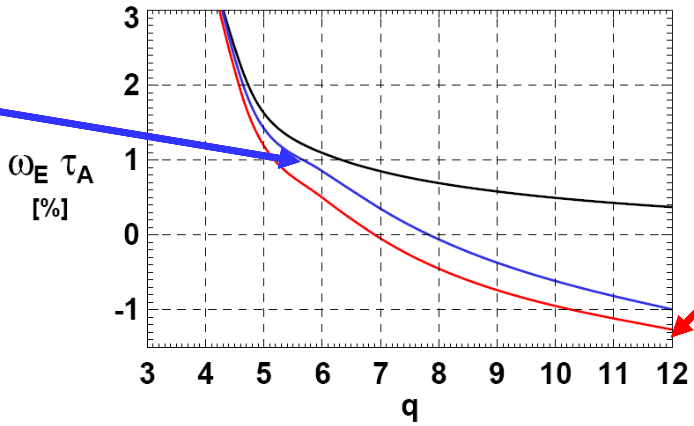

ω_{*C} / ω_{*C} (expt) = 1
u_θ = 0

ω_{*C} / ω_{*C} (expt) = 1
u_θ = neoclassical

Inclusion of v_{pol} in ω_E can sometimes modify marginal stability boundary – example: wall position variation

Calculated n=1 $\gamma\tau_{wall}$

experimentally stable profiles and b_{wall} / a artificially increased × 1.1

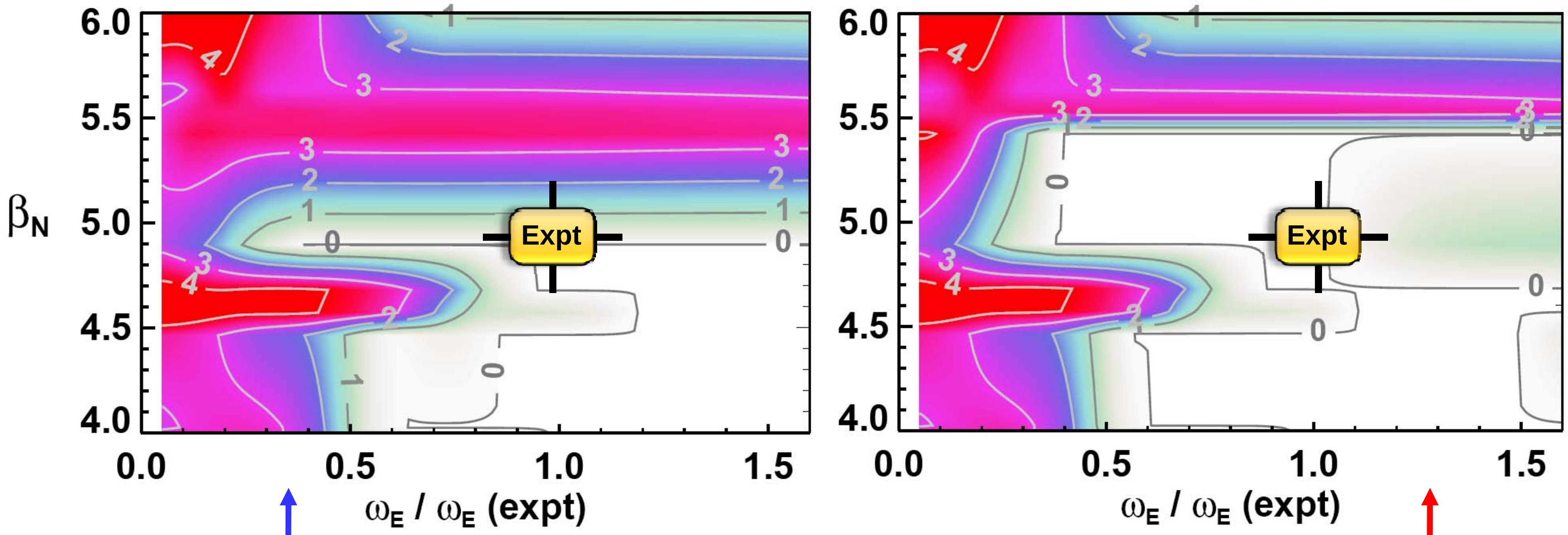

ω_{*C} / ω_{*C} (expt) = 1
u_θ = 0

ω_{*C} / ω_{*C} (expt) = 1
u_θ = neoclassical

- Increased wall distance lowers with-wall limit to β_N ~ 5.5
- Case with u_θ=0 has lower marginal stability limit β_N ~ 5

Kinetic stability analysis using MARS-F

- Experimentally unstable case
- Experimentally stable case
- Comparison of unstable and stable cases

Inclusion of ω_{*C} in ω_E increases separation between stable and unstable $\omega_E(\psi)$ and provides consistency w/ experiment

Toroidal rotation only

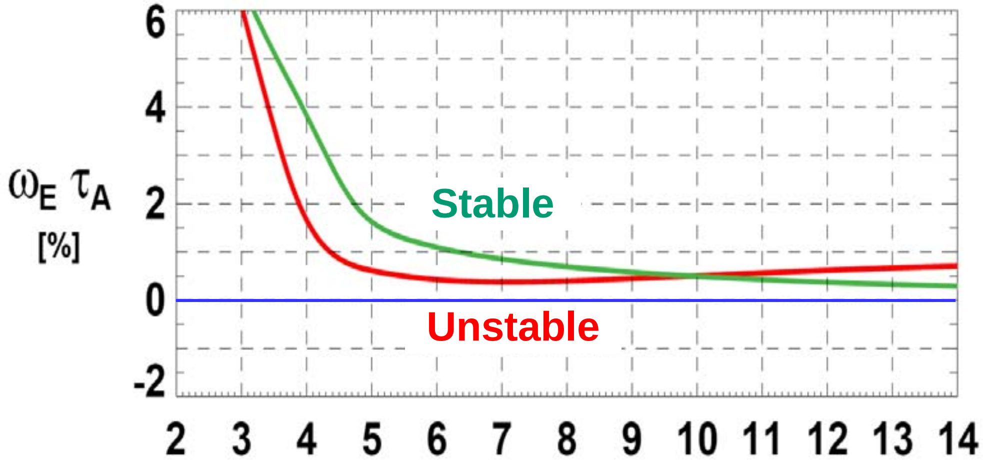

Unstable rotation profile

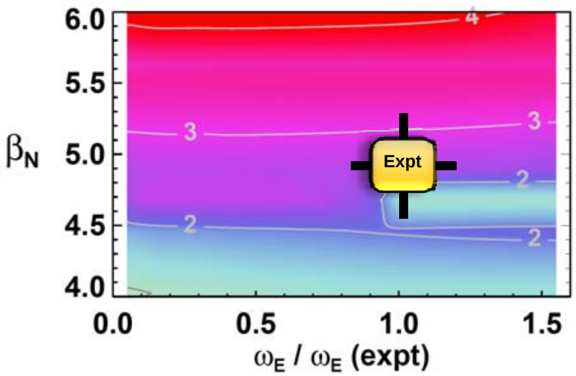

Stable rotation profile

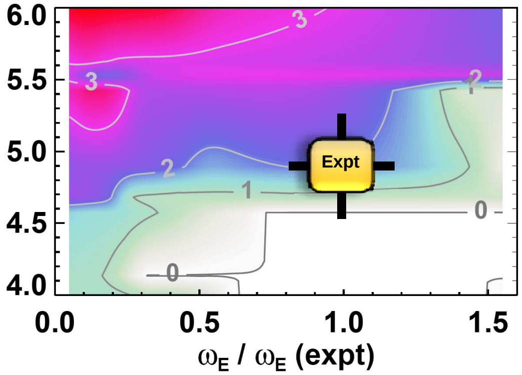

Predictions inconsistent with experiment

Toroidal + diamagnetic

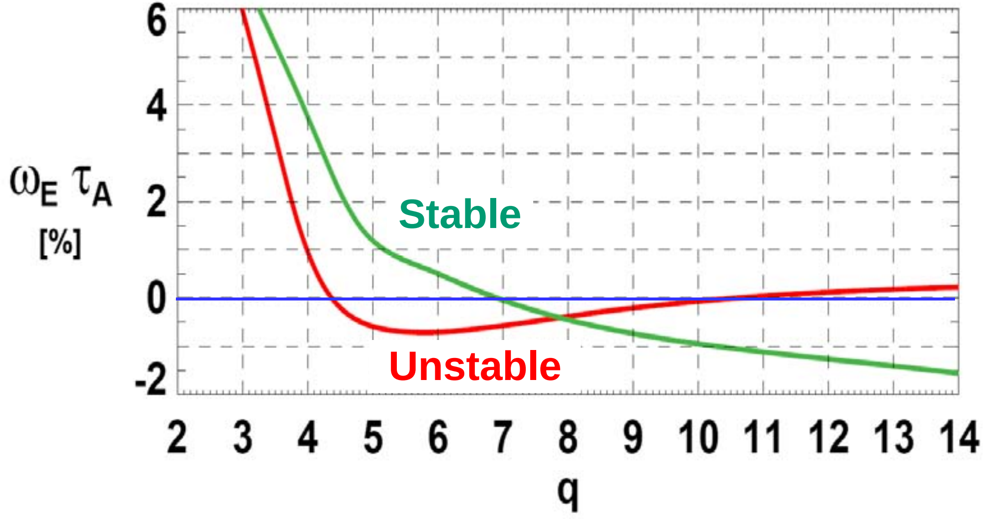

Unstable rotation profile

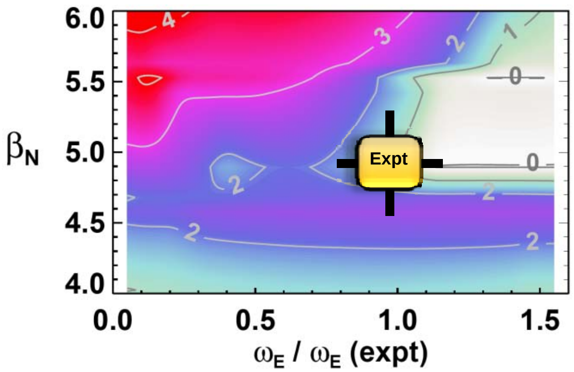

Stable rotation profile

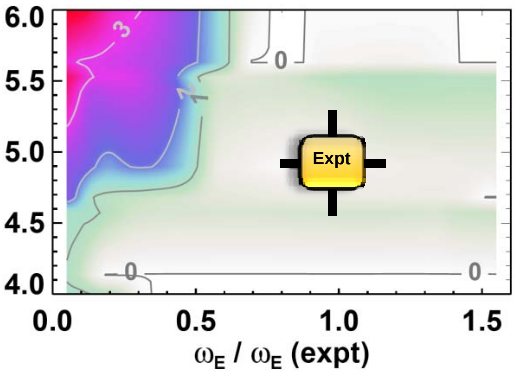

Predictions more consistent with experiment

Mode damping in last 10% of minor radius calculated to determine stability of RWM in n=1 EFC experiments

ω_E / ω_E (expt) = 0.5 used so unstable modes can be identified and local damping computed

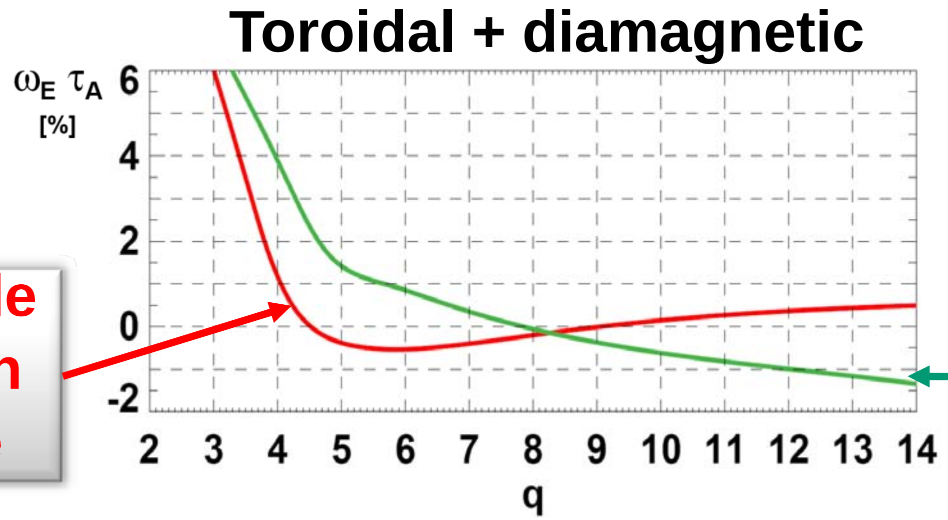

Unstable rotation profile

Stable rotation profile

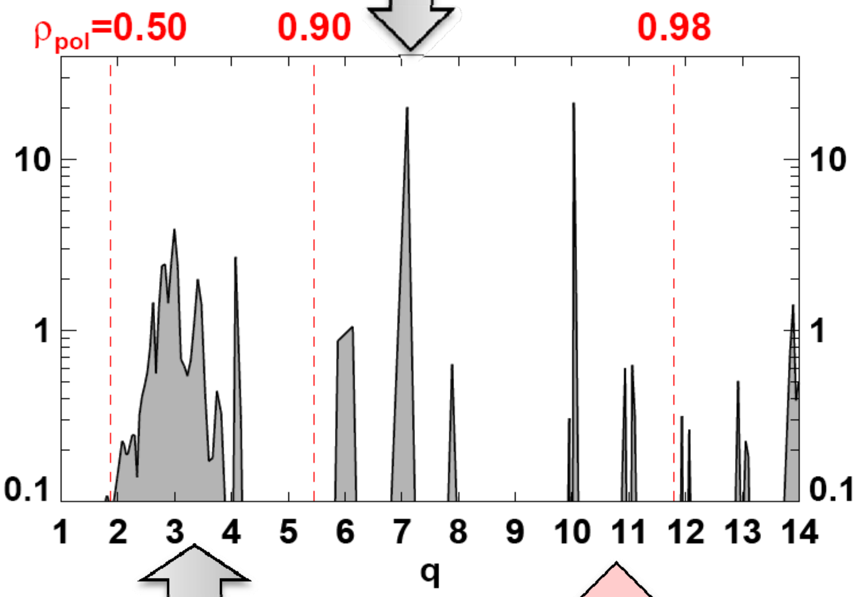

Local mode damping ∝ $\frac{\partial(\delta W_{K\text{-imag}})}{\partial V}$

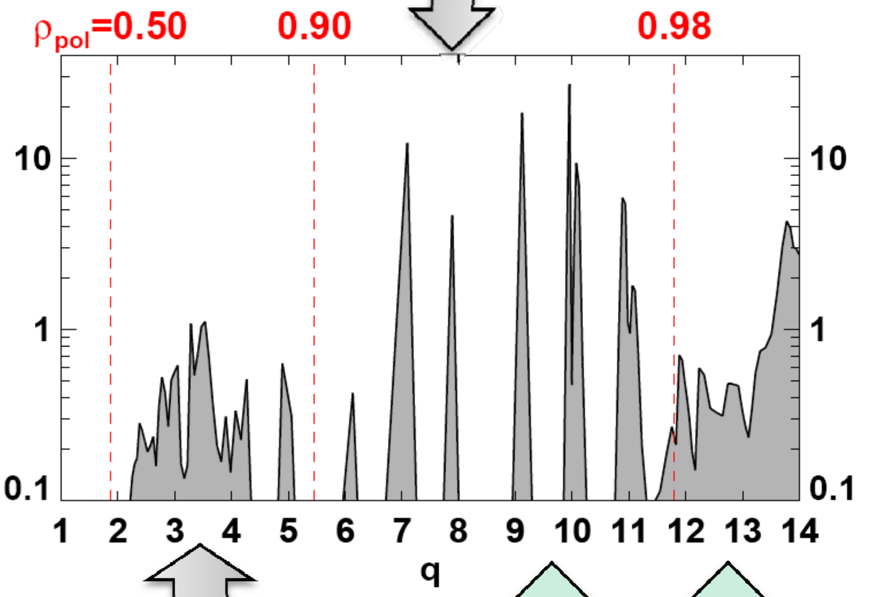

Higher core damping

Lower edge damping

Lower core damping

Higher edge damping

Kinetic stability analysis using MARS-K

- Comparison with experiment
- Self-consistent vs. perturbative approach
- Modifications of RWM eigenfunction

MARS-K consistent with EFC results and MARS-F trends

- MARS-K full kinetic δW_K → multiple modes can be present
  - Mode identification and eigenvalue tracking more challenging
- Track roots by scanning fractions of experimental ω_E and δW_K:

Experimentally unstable case

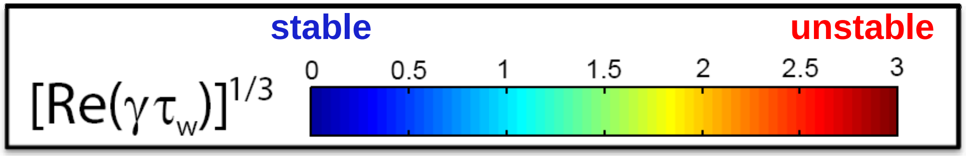

Experimentally stable case

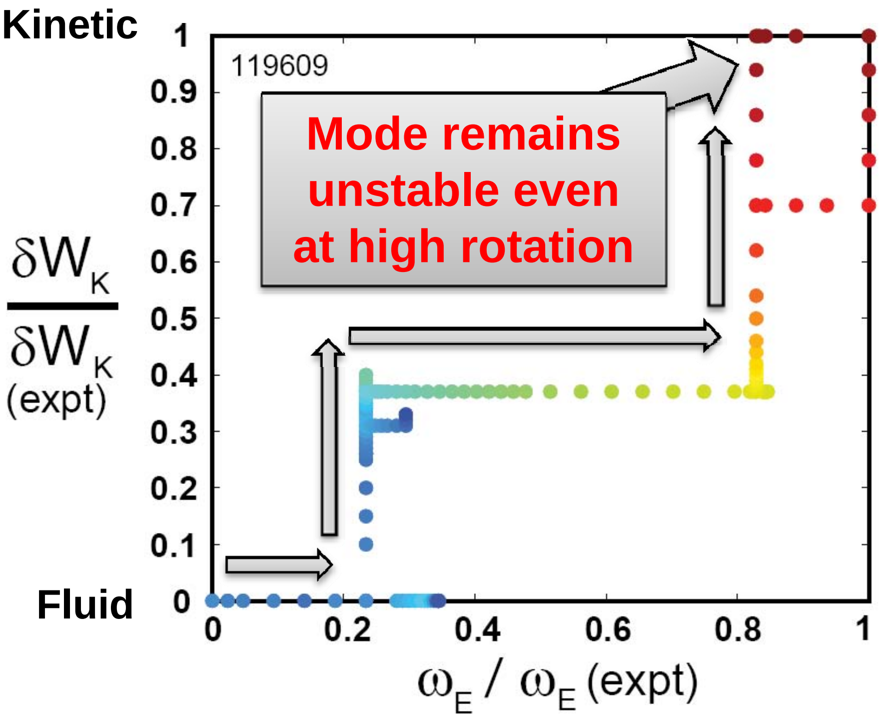

Mode remains unstable even at high rotation

β_N=4.9

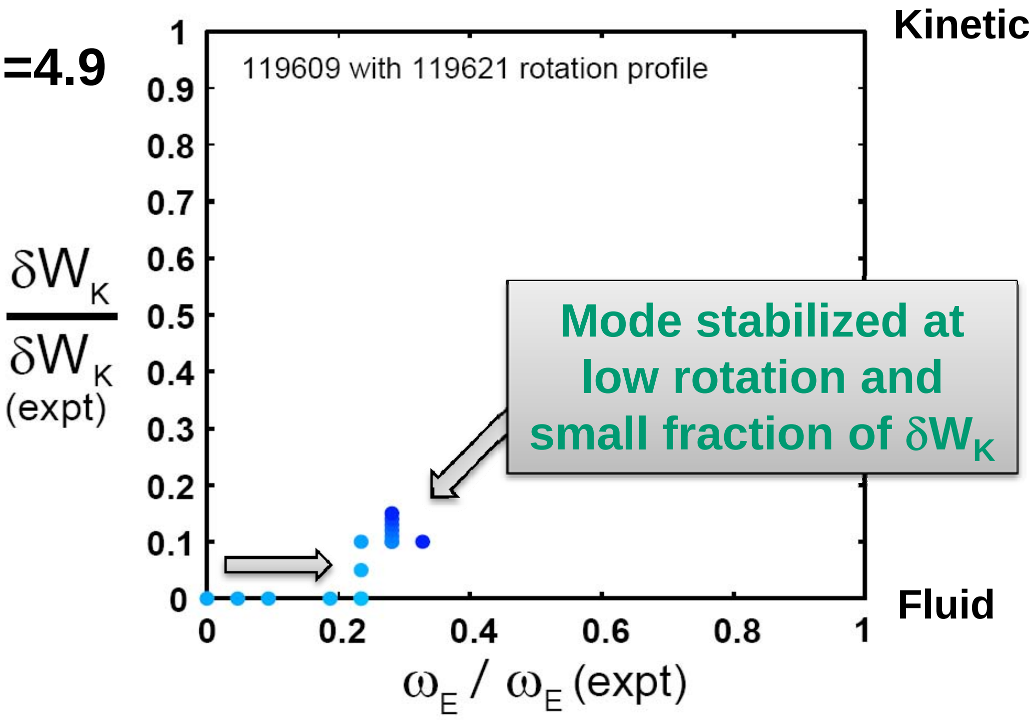

Mode stabilized at low rotation and small fraction of δW_K

Perturbative approach predicts unstable case to be stable → inconsistent with self-consistent treatment and experiment

- Perturbative approach uses marginally unstable fluid eigenfunction at zero rotation in limit of no kinetic dissipation
- For cases treated here, $|\delta W_K|$ can be >> $|\delta W_\infty|$ and $|\delta W_b|$
  - Possibility that rotation/dissipation can modify eigenfunction & stability

Experimentally unstable case

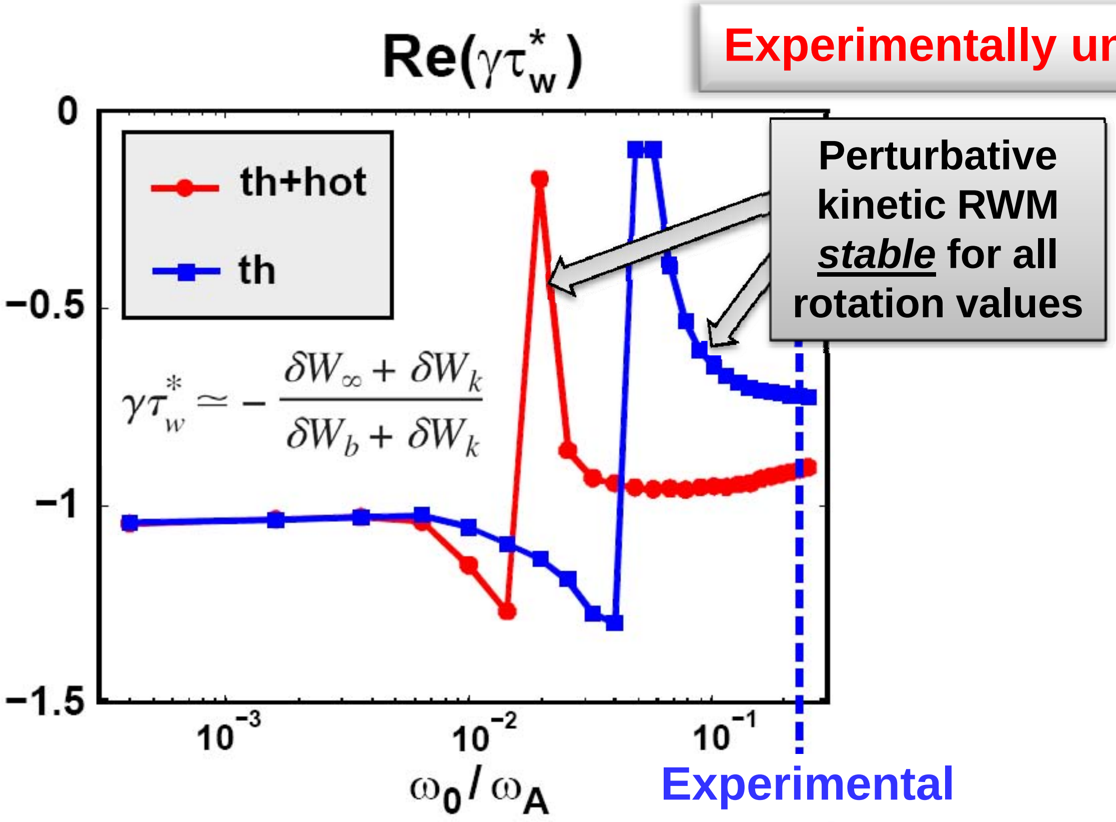

$$\gamma\tau^*_w \simeq -\frac{\delta W_\infty + \delta W_k}{\delta W_b + \delta W_k}$$

Perturbative kinetic RWM ***stable*** for all rotation values

Experimental rotation

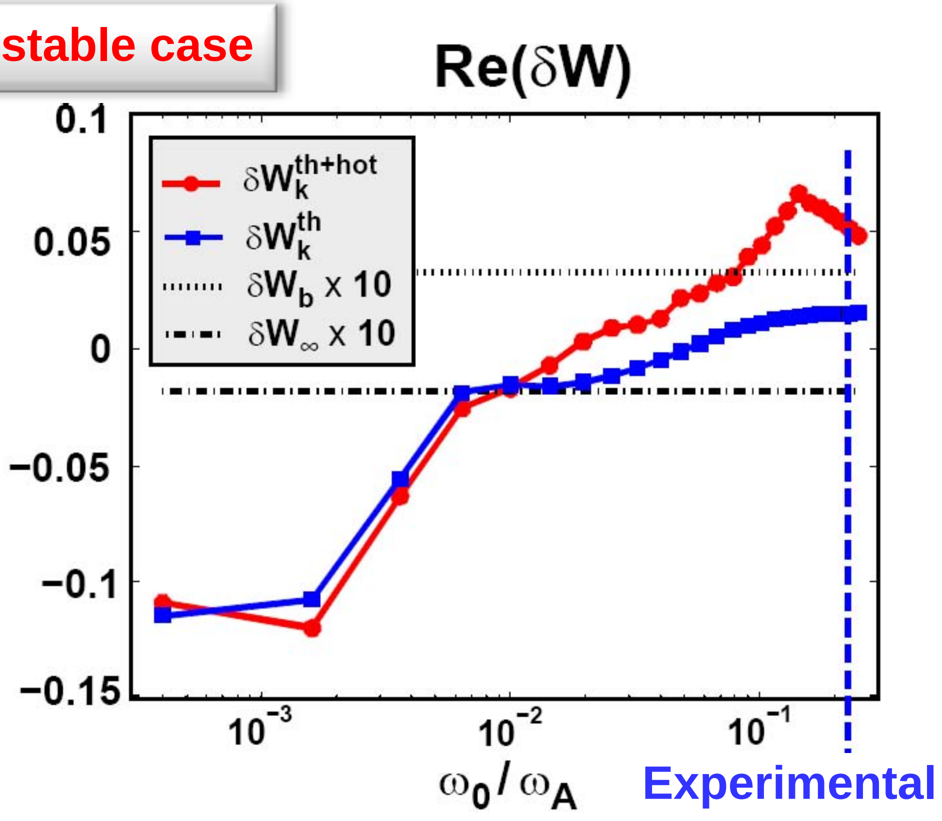

Experimental rotation

MARS-K self-consistent calculations for stable case indicate modifications to eigenfunction begin to occur at low rotation

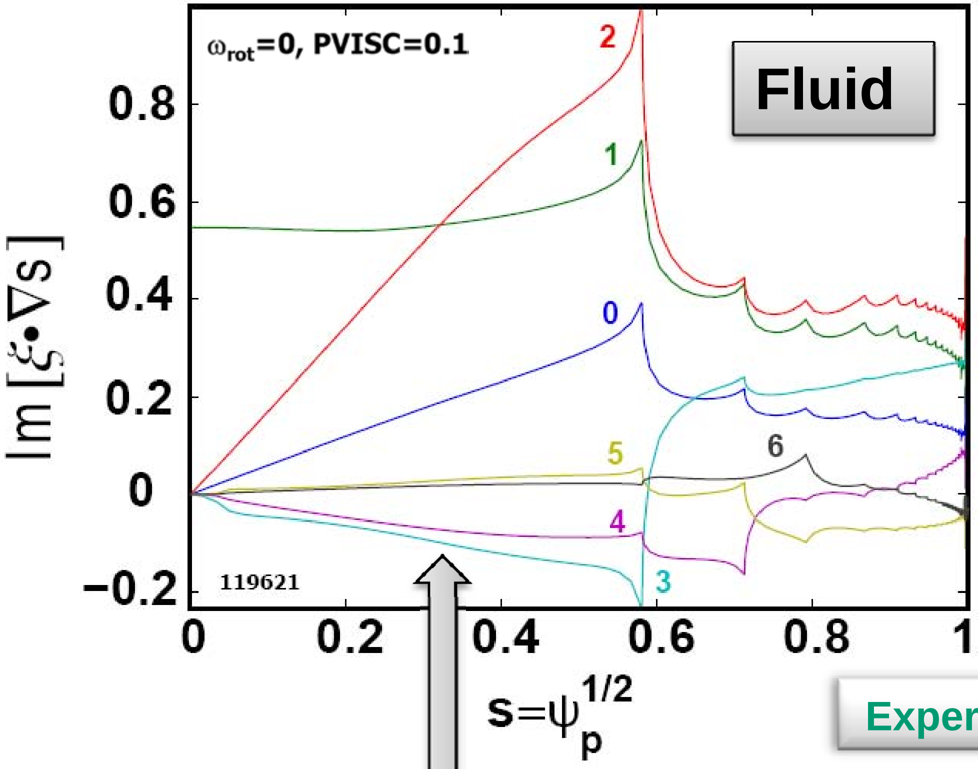

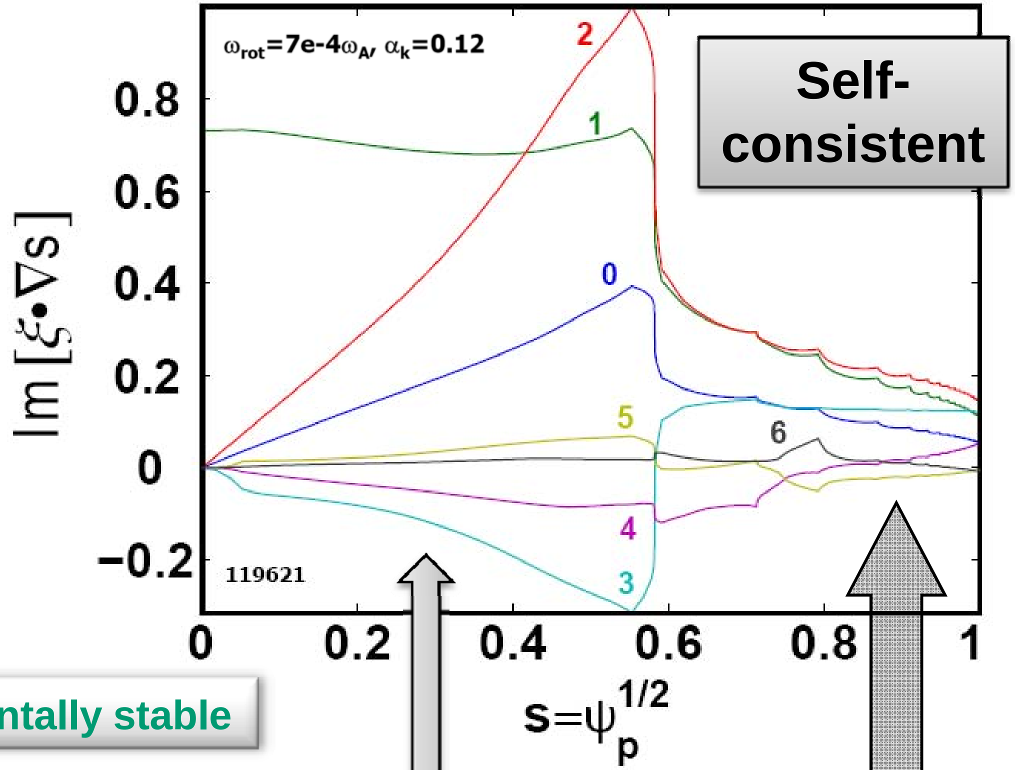

Experimentally stable

- Self-consistent (SC) eigenfunction qualitatively similar to fluid eigenfunction in plasma core
- SC RWM $\xi_\perp$ amplitude reduced at larger r/a
  - Low ω_E / ω_E (expt) = 0.3%, $\delta W_K/\delta W_K$ (expt) = 12%
  - Reduced amplitude could reduce dissipation, stability

MARS-K self-consistent calculations indicate expt. rotation and dissipation can strongly modify RWM eigenfunction

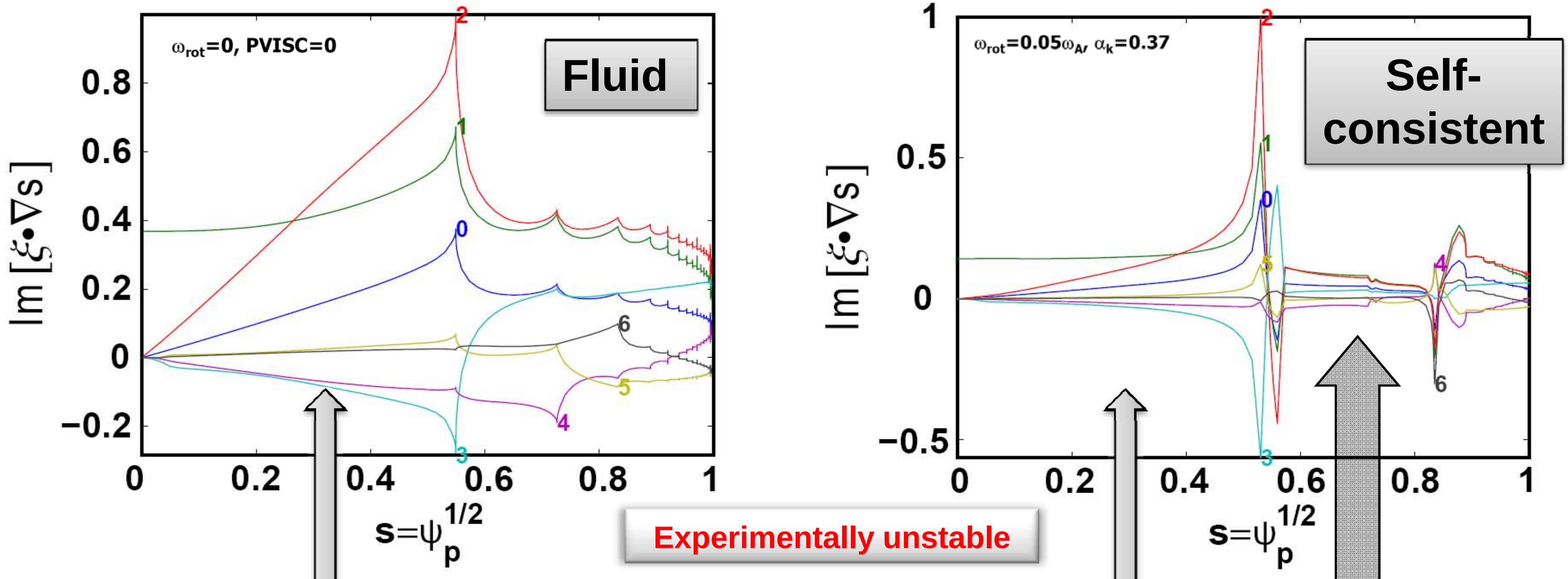

- Self-consistent (SC) eigenfunction shape **differs** from fluid eigenfunction in plasma core
- SC RWM $\xi_\perp$ substantially different at larger r/a
  - Moderate ω_E / ω_E (expt) = 22%, $\delta W_K/\delta W_K$ (expt) = 37%
  - Differences could be even larger at full rotation and δW_K
  - **Does reduced edge $\xi_\perp$ amplitude explain reduced stability?**

Summary

- Edge rotation ($q \geq 4$, $r/a \geq 0.8$) important for RWM
  - Trends consistent with stability calculations using MARS-F
  - Provides insight, method for optimal error field correction
- Stability quite sensitive to edge ω_E profile
  - Essential to include accurate edge ∇p in E_r profile
  - Poloidal rotation can also influence marginal stability
- Full kinetic stability (MARS-K) consistent w/ experiment
- Perturbative treatment inconsistent – overly stable
  - Edge eigenfunction strongly modified by rotation/dissipation
  - Reduction in $\xi_\perp$ amplitude may reduce kinetic stabilization